Available online at www.sciencedirect.com
SCIENCE DIRECT®
Catalysis Today 98 (2004) 151–160
CATALYSIS TODAY
www.elsevier.com/locate/cattod

Effect of alumina preparation on hydrodemetallization and hydrodesulfurization of Maya crude

Mohan S. Rana*, J. Ancheyta, P. Rayo, S.K. Maity

Instituto Mexicano del Petróleo, Eje Central Lázaro Cárdenas 152, Mexico City 07730, Mexico

Abstract

Hydrodesulfurization (HDS) and hydrodemetallization (HDM) of Maya crude were carried out in a high pressure (5.4 MPa) micro-reactor close to industrial practice. The effect of support preparation (γ-alumina) was compared using different preparation techniques. The different support preparation methods leading to a variation in textural properties of the supports and its characterization provides important information about their applicability for Maya crude processing. Ammonium carbonate prepared supports provide improved pore size distribution as well as high pore volume. The prepared catalysts are effective for HDS and HDM, having less formation of deteriorating substances such as Ni and V with more stable behavior against time-on-stream. The HDM activity increases while the HDS activity decreases with increasing average pore diameter. Laboratory prepared catalysts showed comparable performance as well as stability in comparison with commercial catalysts against hydrotreating of heavy Maya crude feed. Among all prepared catalysts, better porosity containing catalysts represent higher and stable activity for HDM as a function of time-on-stream. The comparison of catalyst activity was carried out with commercial one which contains TiO_2 and higher amount of molybdenum. The results of activity and stability of catalyst protrude distinct contribution of pore size distribution of support which has more capabilities to retain metal deposition as well as better diffusion of complex organo-chelating metals (V, Ni, etc.).

Keywords: Hydrotreating catalyst; Alumina support; Pore size distribution; HDM; HDS

1. Introduction

Refineries in the world currently have the capability to produce ultra-low sulfur diesel containing less than 50 wppm. It was realized that EPA specification of 500 wppm sulfur (5000–500 wppm, 1993) was easier than anticipated [1]. In contrast, the further specification as low as 15 wppm represents a new and far more challenging task for the researcher as well as industry, because the remaining refractory sulfur (less than 500 wppm) is likely to be contained in compounds that are difficult to desulfurize, generally described as sterically hindered sulfur containing molecules. Furthermore, to meet the growing demand of clean fuels, the implications are complex, not only from a highly active catalyst but also from a refinery stand-point. Each refinery has unique circumstances, such as source of crude, diesel blend components and hydrogen availability. Moreover, production of light petroleum is decreasing day by day and refiners and researchers are concentrating accordingly on processing and/or improving the heavier feedstock, making the task more complicate.

Crude oils are mixture of virtually infinite number of different hydrocarbon molecules; such as paraffins, naphthenes, asphaltenes and aromatics together with molecules containing hetero-atoms; the later being mainly sulfur, nitrogen, vanadium and nickel. The content of these heteroatoms in petroleum varies as a function of the source of crude oils and refinery location. The following data are examples of the heteroatoms content in heavy feedstocks: Maya crude (Mexico) contains ∼330 wppm Ni + V and ∼3.3 wt.% S, while Boscan crude (Venezuela) contains ∼340 wppm Ni + V and ∼5.5 wt.% S. Generally, the metal atoms (Ni, V, etc.) are present in the form of porphyrins or chelating compounds and during the hydrocarbon conversion process these metals are deposited on the catalyst as

* Corresponding author. Tel.: +52 55 9175 8418; fax: +52 55 9175 8429.
E-mail address: msingh@imp.mx (M.S. Rana).

0920-5861/$ – see front matter © 2004 Elsevier B.V. All rights reserved.
doi:10.1016/j.cattod.2004.07.029

metal sulfides (Ni_3S_2, V_3S_4 and V_2S_3, etc.) crystallite ranging from 2 to 30 nm in size [2]. These transition metal sulfides poison the catalysts by decreasing the catalytic active sites and hinder the transportation of reactant as well as eventually block the pores. Normally, the mineral metals such as Mg, Ca and Fe sulfides are deposited on the exterior surface of catalysts, while the Ni and V sulfides are generally deposited throughout the catalyst [2,3]. The heavy feedstocks also contain significant amount of asphaltene, which are the heaviest component and equally responsible for catalyst deactivation in hydroprocessing along with metal deposition [4–6]. Since the molecular size of asphaltenes exceed more than 2 nm [7], it has been accepted that mesoporous (2–50 nm diameter) catalyst supports for hydrotreating of heavy feeds play an important role in efficient processing and consequent avoidance of catalyst deactivation [4,8–11].

The present investigation is an attempt to develop suitable catalyst for Maya crude hydrotreating using different preparation methods for γ-alumina support with better textural properties as well as more resistance to metal tolerance. In order to draw the concept governing the support preparation in hydrotreating catalyst performance various methods were used for alumina support preparation, mainly focused on the variation of porosity and pore size distribution. The activity tests were carried out with real feedstocks having conditions very close to industrial practice and the catalytic results were compared with NiMo commercial catalysts. The HDS and HDM results of prepared catalysts are discussed under the nature of pore structure, metal deposition and the characterization techniques.

2. Experimental

Pure alumina supports were prepared by using different preparation methods such as urea, ammonium carbonate and ammonia as hydrolysing agents.

Urea hydrolysis method was used for the homogeneous precipitation method employing aluminum nitrate solution (∼1.5 M) and 500 g of urea. The preparation flow diagram is given in Scheme 1. The solution was refluxed at about 95 °C (±3 °C) for 10 h (controlling the pH of precipitate ≈7.5–8.5), to allow precipitation of aluminium hydroxides. The milky white precipitate appears during the refluxing at the above said temperature. The precipitate was aged over night (10 h) and filtered, washed; the precipitate was dried overnight at 120 °C. A sample prepared by urea hydrolysis is represented as γ-Al_2O_3-u.

Ammonium carbonate and aluminum nitrate solutions were mixed together simultaneously (one step swing method) and the pH was controlled at ∼8 using ammonium carbonate solution, the mixing (stirring) starts at room temperature, after 30 min the precipitate was heated up to 95 °C and refluxed in presence of stirring for 4 h. The final pH of solution was maintained at 8.0. The precipitated solution was aged at room temperature for 10 h. The aged solution was filtered and washed and then dried at 120 °C. The flow diagram is presented in Scheme 2. The sample is represented as γ-Al_2O_3-acs (ammonium carbonate swing method).

Another support of γ-Al_2O_3 was prepared by slow addition of ammonium carbonate with continuous stirring and controlled pH ∼8.0. The solution precipitate was refluxed at 95 °C for 4 h. The precipitated solution was aged at room temperature for 10 h. The aged solution was filtered, washed and dried at 120 °C. This support is assigned as γ-Al_2O_3-ac (ammonium carbonate).

γ-Al_2O_3 support was prepared by co-precipitation method using aq. NH_3 solution (≈5%) for aluminium nitrate (1.5 M) precipitation at constant pH of 8.0 with continuous stirring at room temperature for 4 h. The flow diagram of preparation is given in Scheme 3. The support is represented as γ-Al_2O_3-am. The above prepared supports were calcined finally at 550 °C for 4 h.

The molybdenum-supported catalysts were prepared by the incipient wetness impregnation method. An appropriate amount of ammonium heptamolybdate (AHM) (Fluka AR grade) was dissolved in ammoniac solution for impregnation. The Co- and Ni-promoted catalysts were also prepared by sequential impregnation procedure on Mo-loaded catalysts (dried at 120 °C and calcinced at 400 °C). The cobalt and nickel nitrate salts were impregnated in aqueous medium. The final catalysts were dried in presence of air at 120 °C overnight and calcined at 450 °C for 4 h. The compositions of catalysts are reported in Table 1.

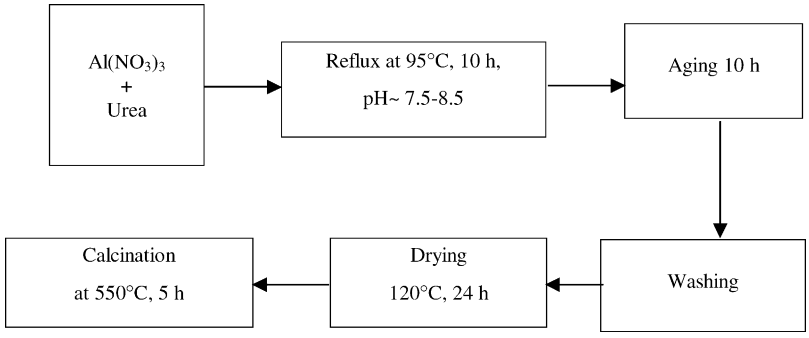

Scheme 1. Flow diagram of γ-Al_2O_3 preparation using urea as a hydrolyser.

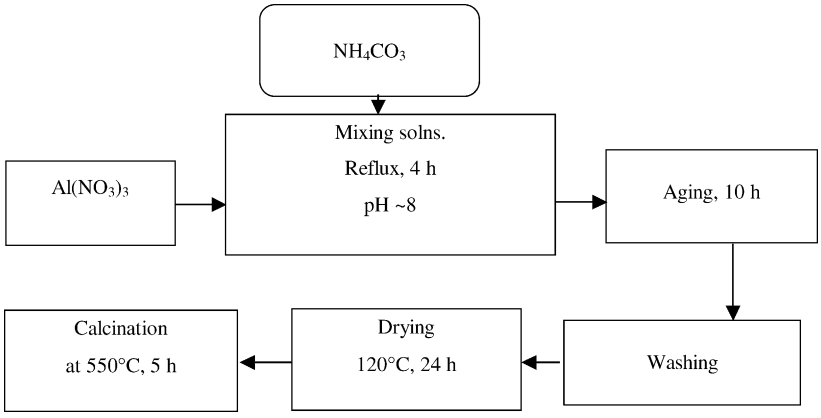

Scheme 2. Flow diagram of γ-Al_2O_3 preparation using ammonium carbonate as a hydrolyser.

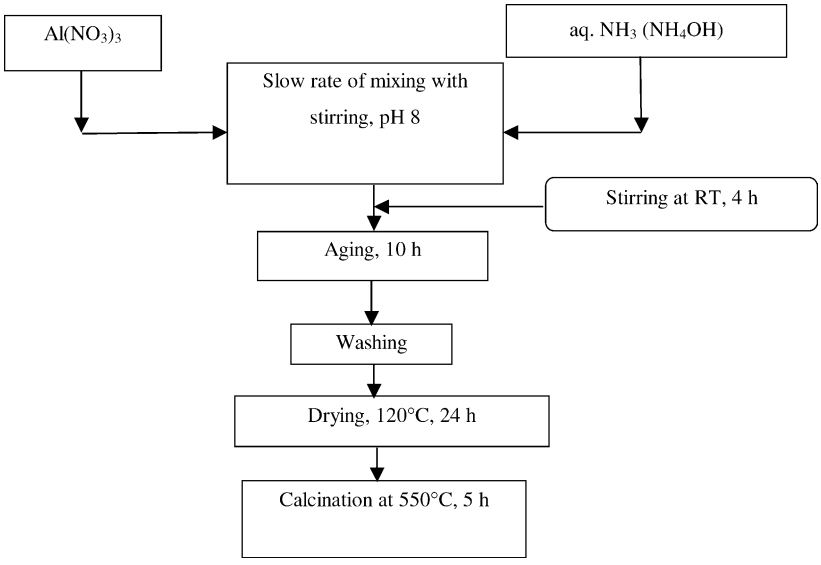

Scheme 3. Flow diagram of γ-Al_2O_3 preparation using ammonium hydroxide as a hydrolyser.

Table 1
Catalysts characterization and composition

Catalysts	Support textural properties			Catalysts textural properties			Composition (wt.%)	
	SSA (m^2/g)	PV (ml/g)	APD	SSA (m^2/g)	PV (ml/g)	APD (nm)	Mo	Co (Ni)
HDS feed								
CoMo/γ-Al_2O_3-ac	215	0.45	8.2	201	0.37	6.0	7.3	2.5
NiMo/γ-Al_2O_3-am	181	0.31	7.0	164	0.27	6.4	7.8	(2.4)
CC-1[a]	–	–	–	188	0.47	9.6	11.4	(2.9)
HDM feed								
CoMo/γ-Al_2O_3-u	158	0.52	15.0	136	0.39	12.9	7.5	2.5
CoMo/γ-Al_2O_3-acs	183	0.63	16.3	160	0.47	17.3	6.8	2.5
CoMo/γ-Al_2O_3-am	181	0.31	7.0	169	0.27	6.5	7.5	2.5
CC-2[b]	–	–	–	175	0.56	15.2	10.6	(2.8)

APD: average pore diameter.
[a] Commercial catalyst for HDS feed, γ-Al_2O_3 + Ti 5.6 wt.%.
[b] Commercial catalyst for HDM feed, γ-Al_2O_3 + Ti 3.7 wt.%.

The BET specific surface area (SSA), pore volume (PV) and pore size distribution (PSD) were carried out in a Quantochrome Nova 2000 equipment. Nitrogen gas was employed for SSA measurements at liquid nitrogen temperature (−196 °C). Prior to the adsorption, the samples were degasses 3 h at 300 °C. X-ray power diffraction (XRD) patterns were collected on a Siemens D500 diffractometer in a 2θ range 5–70° at 2.5°/min scan rate using Cu Kα radiation.

To evaluate the catalytic behavior with real feed the catalysts were tested in a high pressure micro-reactor in up flow mode described elsewhere [12–14] against HDS and HDM feeds. The HDS feed was prepared synthetically using a 50/50 (w/w) composition of partially pre-hydrodemetallized (HDM) Maya crude and diesel while the HDM feed contains 50/50 (w/w) of Maya crude and diesel. Diesel was used as a solvent or diluent to avoid precipitation as well as gum formation during the feed processing. The properties of the feed are presented in Table 2. The pre-HDM Maya crude with diesel is called HDS feed and pure Maya crude with diesel is known as HDM feed. Metals (Ni, V) were analyzed in the feed and products using flame atomic adsorption spectrometry (ASTM D 5863-00a method). The total S content was analyzed by ultra-violate fluorescence (ASTM D 5453-00 method) while nitrogen was measured by oxidative combustion and chemiluminescence (ASTM D 4629-02 method) at high temperature combustion in an oxygen rich atmosphere. Asphaltene is defined as the insoluble fraction in *n*-pentane. The solid carbonaceous material on spent catalysts (toluene washed) was analyzed with a Leco SC-444 instrument using ASTM: C 1408-98 method by direct combustion-infrared detection.

The catalyst pretreatment and the hydrotreating reactions were carried out in the high pressure fixed-bed up flow micro-reactor. The catalyst was sulfided in situ with a mixture of dimethyldisulfide (DMDS), straight run gas oil (SRGO) and H_2. The H_2S is produced by decomposition of DMDS in situ. The reactor was loaded with 10 ml (∼7 g) of oxidic catalyst with 3–5 mm extrudate size diluted with equal volume of SiC. After de-pressurizing the reactor to atmospheric pressure, the sulfiding feed (1 wt.% DMDS + SRGO) containing ≈2.0 wt.% "S" was started to wet the catalyst bed at room temperature. The liquid was drained after 4 h, and then the temperature was linearly rose from 30 to 120 °C (30 °C/h) and kept at this temperature for 2 h. Later, the temperature was increased at the rate of 30 °C/h until 150 °C, at 2.8 MPa pressure and stayed 2 h, further increase of temperature at 260 °C and dwelled for 3 h. The final temperature of sulfidation was 320 °C, which was stabilized for 5 h at 2.8 MPa. After sulfidation, the flow was switched to HDS or HDM feed (Table 2) and the following operating conditions were adjusted: temperature of catalyst bed 380 °C, LHSV of 1 h^{-1}, H_2/HC 356 m^3/m^3 and pressure of 5.4 MPa [15].

Table 2
Characterization and composition of HDS and HDM feeds

Properties	HDS[a]	HDM[b]
Elemental analysis		
C (wt.%)	83.2	84.2
H (wt.%)	9.5	8.8
N (wt.%)	0.133	0.184
S (wt.%)	0.841	2.21
Metal (wppm)		
Ni	25.04	26.21
V	86.84	124.78
(Ni + V)	111.88	150.99
Asphaltene (wt.%) (*n*-C5 insol.)	6.36	8.43
Physical properties		
Density (20/4 °C)	0.8505	0.88
Pour point (°C)	−24	−15
Ramscarbon (wt.%)	4.29	5.45
Viscosity (g/cm s)		
At 50 °C	2.63	3.08
At 100 °C	8.29	9.45

[a] Maya HDM/diesel (50/50 (w/w)).
[b] Maya crude/diesel (50/50 (w/w)).

3. Results and discussion

3.1. Supports pore volume and pore size distribution

For the γ-Al_2O_3 preparation from aqueous solutions of aluminum nitrate and urea in which precipitant is produced in situ, hydrolysis is kinetically controlled by slowly generated –OH ions through urea decomposition to NH_3 and CO_2. Fundamentally, the precipitation technique involves the physical as well as chemical processes. The precipitant is added indirectly to the solution at a temperature in to vicinity of ∼95 °C, which allows to proceed the precipitation internally and homogeneously, resulting into more control over the pore volume and macro-pore size distribution. However, the different parameters such as aging time, pH, precipitating agents, concentration of solution, etc., play an important role to generate the textural properties of support. At synthesis conditions the most probable phase of boehmite and pseudoboehmite is aluminum oxyhydroxide [AlOOH]. These trivalent ions of oxyhydroxides are having capacity to retain the bulky component between the layers. The γ-Al_2O_3-acs showed similar type of pore size distribution but pores >50 nm is slightly increased and remain constant up to 200 nm. A plausible explanation for this increase is that during the precipitation the CO_3 is trapped in a bulk between the aluminum oxyhydroxide [AlOOH] with layered type of material, which escaped during the calcinations and provides larger porosity and improved pore size distribution (PSD). The γ-Al_2O_3-ac and γ-Al_2O_3-am represents a similar profile for N_2 adsorption showing maximum PSD in the range of 5–10 nm. In this method the carbonate could not represent similar behavior may be due to the atomic precipitation, which could not retain the CO_3 molecule between the layers of [AlOOH]. Similar kind of PSD can be seen with

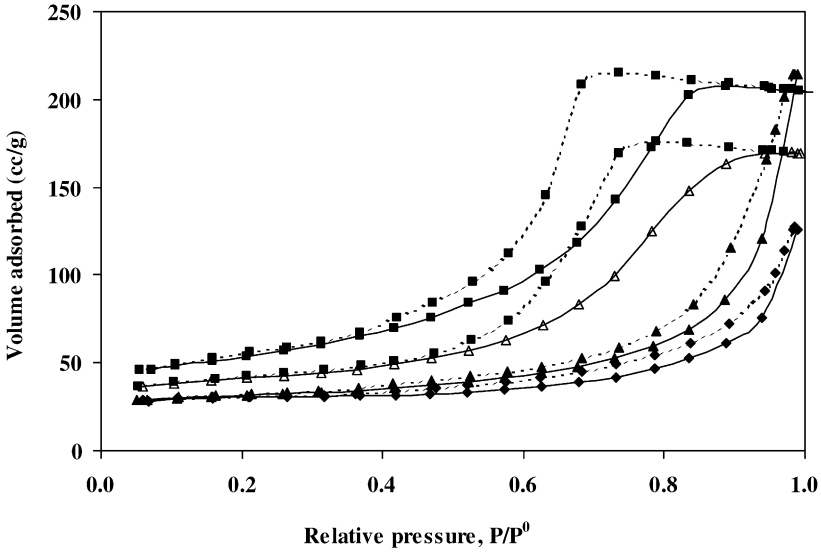

Fig. 1. N_2 adsorption (solid)–desorption (dotted) isotherm of γ-Al_2O_3 supports: (◆) γ-Al_2O_3-u; (▲) γ-Al_2O_3-acs; (△) γ-Al_2O_3-ac; (■) γ-Al_2O_3-am.

NH_4OH precipitation, thus, the later two methods behave in an identical way.

The comparative nitrogen adsorption–desorption isotherm of supports at −196 °C can be observed in Fig. 1. The ammonia and carbonate (slow precipitation) prepared alumina exhibited a Type IV isotherm, indicative of meso-porosity. The other two supports exhibited a Type II isotherm suggesting almost no micro- or meso-porosity. These different isotherms represent the typical characteristics [16] of sample for example: (i) a slow increase in nitrogen uptake at low relative pressure (P/P^0) which corresponds to the monolayer-multilayer adsorption on the pore walls; (ii) a sharp step at intermediate relative pressure representing the capillary condensation within meso-porous; (iii) a plateau with a slight inclination at high relative pressure associated with multilayer adsorption on the textural surface of the crystal; (iv) the characteristic of a sharp rise in N_2 uptake at relative high pressure ($P/P^0 \approx 0.9$), attributed to the condensation of nitrogen with in void form by crystal aggregation as shown in γ-Al_2O_3-u and γ-Al_2O_3-acs isotherms.

3.2. Catalysts characterization

The pore size distributions of supported catalysts along with two commercial catalysts are presented in Fig. 2a and b. The data were derived after CoMo impregnation from N_2 adsorption isotherms. The lab prepared catalysts showed mono-modal type of pores while commercial catalysts contain bi-modal type of porosity. The CoMo/γ-Al_2O_3-acs and CoMo/γ-Al_2O_3-u supported catalysts showed greater number of pores toward macro-size diameter, while CoMo/γ-Al_2O_3-am, NiMo/γ-Al_2O_3-am and CoMo/γ-Al_2O_3-ac catalysts exhibit only meso-pores after active metal impregnation. On the basis of these pore size distributions the catalysts can be selected for the HDM and HDS feeds processing.

The XRD results of pure γ-Al_2O_3 support and CoMo supported catalysts (Fig. 3) do not give any information about the active metal crystallization, which might be due to the low loading of Mo on supports. Spent catalyst (after 60 h time-on-stream) X-ray diffractogram carried out in order to see the metal (Ni and V) deposition on the outer surface of catalyst is also shown in Fig. 3. The metals exist as the sulfide compounds and are shown in the X-ray diffraction pattern as the V_3S_4, V_2S_3 and Ni_3S_2 phases. The Ni_3S_2 phase does not appear visible may be due to the crystallite size less than 4 nm. The majority of sulfided phase can be seen and compared with the standard values of the Joint Committee on Powder Diffraction Standards (JCPDS) [17] for V_3S_4, V_2S_3 and Ni_3S_2 crystallites. In general, the metal deposited layer is coated on the wall of cylindrical pores, thus, the pore diameter continuously decreases with metal deposition or time-on-stream. In different characterization studies, carried out by Smith and Wei [18–20] (TEM, EDX, STEM and PS) for the HDM of model molecules on deactivated catalyst and by Takuchi et al. [21] (XRD, ESR and SEM) on the catalysts used in hydrodemetallization of heavy oil, the V_2S_3 phase was observed in acicular or rod shaped crystallites about 100 nm in length. Toulhot et al. [22] reported that nickel is always associated with vanadium [Ni(V_3S_4)] and its crystallite size ranged from 5 to 30 nm, which grew perpendicular to the alumina platelets.

3.3. Activities and selectivity

The supported catalysts activity tests were carried out in high pressure micro-plant with Maya crude and diesel mixture. After diesel dilution the crude oil continues being a

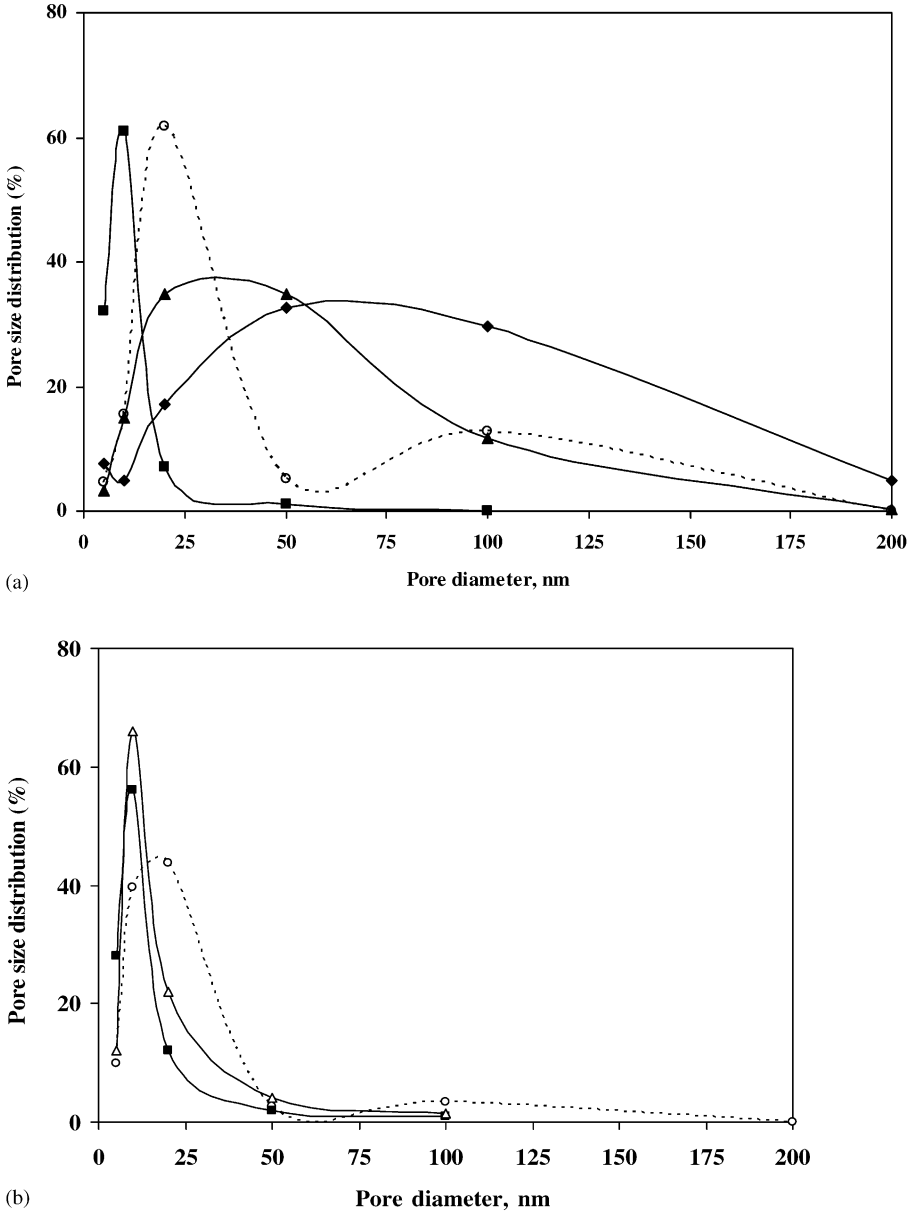

Fig. 2. Pore size distribution of supported catalysts: (a) (◆) CoMo/γ-Al_2O_3-u; (▲) CoMo/γ-Al_2O_3-acs; (■) CoMo/γ-Al_2O_3-am; (○) CC-2; and (b) (△) CoMo/γ-Al_2O_3-ac; (■) NiMo/γ-Al_2O_3-am; (○) CC-1.

mixture of several heavy fractions with metalloidal (V, Ni, etc.) compounds and asphaltenes. The feeds specifications are reported in Table 2. On the basis of catalysts porosity and PSD they are tested against the different feeds as described below.

3.3.1. HDS feed

The catalytic activities for hydrodesulfurization and hydrodemetallization with HDS feed are shown in Figs. 4 and 5, respectively. The results of activity are compared with the CC-1 commercial catalyst, with the properties presented in Table 1. The lab prepared alumina supported catalysts showed much higher as well as stable activity than the commercial catalyst as a function of time-on-stream. The CoMo/γ-Al_2O_3-ac supported catalyst represents more stable and better HDS activity due to the high specific surface area that may result in better dispersion of Mo phase, while the NiMo/γ-Al_2O_3-am results are slightly lower than the previous one. The unstable behavior with time-on-stream showed by commercial catalyst may be due to the presence of TiO_2 which generates some acid sites on the catalyst surface and as a result activity decreases faster than pure alumina supported catalyst which is known to be more stable and conventional catalyst support for hydrotreating [3]. Eijsbouts et al. [23,24] suggested that HDS deactivation is due to the loss of the active phase dispersion while Gosselink [2] reported that during heavy oil hydro-conversion the metal sulfide deposition is taking place on the pore mouth; thus an increment in the pore diameter increases the

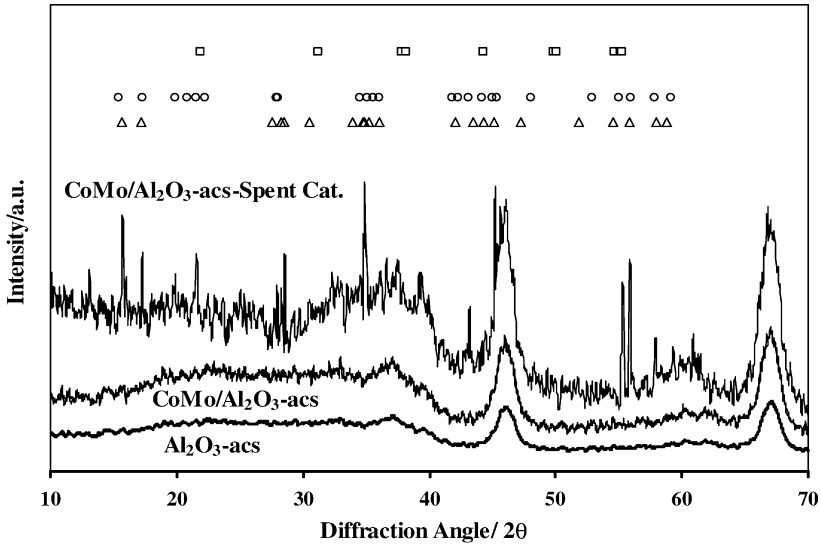

Fig. 3. X-ray diffraction patterns for γ-Al_2O_3 support, catalyst, spent catalysts and comparison with JCPDS-ASTM data: (△) V_3S_4; (○) V_2S_3 and (□) Ni_2S_3.

metal tolerance, but decreases the surface area and the activity. Hence, the HDS of heavy oil is a balance between two independent parameters.

The HDM activity of lab CoMo prepared catalyst (Fig. 5) is more stable than the commercial catalyst which has bimodal type of pore size distribution. Therefore, with a low sever feed, i.e. HDS feed, hydrodemetallization is more facile to the active site of catalyst in which Co-Mo catalyst is more stable and better than NiMo catalyst as well as than commercial catalyst which also contains Ni. The NiMo/γ-Al_2O_3-am supported catalyst has low pore volume and PSD (meso-pore) in the range of 5–20 nm and consequently its activity is limited due to the penetration of complex metal containing molecules (porphyrins or metal chelating compounds) into the pores. However, better activity of HDS was observed with both lab prepared catalysts which further gave an idea about the pore restriction in which sulfur molecule is comparatively smaller than metal containing molecules and can be easily diffuse into the smaller pores.

The selectivity of catalysts is shown in Fig. 6. The HDS and HDM selectivities are plotted against hydrodearomatization of asphaltene (HDAs), which indicates that the HDAs activity follows similar tendency to HDM that might be due to the diffusion of asphaltene molecules into the pores.

3.3.2. HDM feed

The hydrodemetallization and hydrodesulfurization activities with HDM feed are reported in Figs. 7 and 8, respectively. The HDM activity decreases with time-on-stream in similar magnitude for all catalysts including commercial one. However, the CoMo/γ-Al_2O_3-acs supported catalyst showed slightly better performance than the others. The activity deficit is clearly due to the metal poisoning on the catalyst surface. The metal (V and Ni) deposition is also supported by the XRD (Fig. 3) and pore size distribution characterization results. The pore size distributions carried out on CoMo/γ-Al_2O_3-acs fresh and spent catalysts are shown in Fig. 9. It is clear from this figure

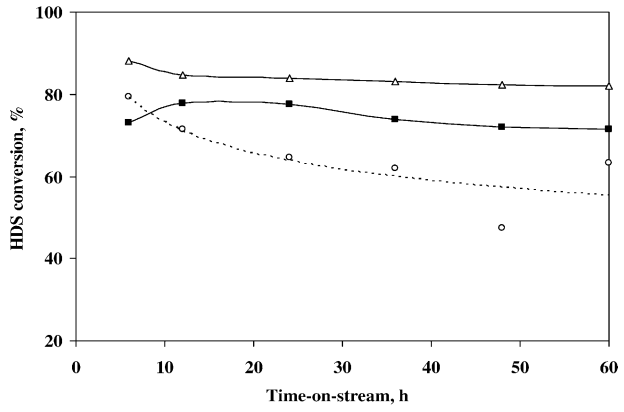

Fig. 4. HDS conversion with time-on-stream: (△) CoMo/γ-Al_2O_3-ac; (■) NiMo/γ-Al_2O_3-am; (○) CC-1.

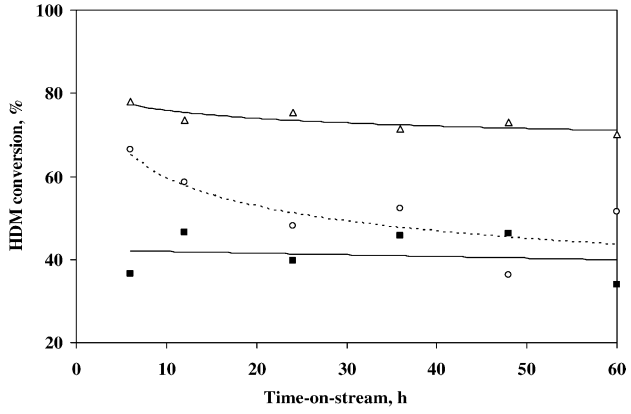

Fig. 5. HDM conversion with time-on-stream: (△) CoMo/γ-Al_2O_3-ac; (■) NiMo/γ-Al_2O_3-am; (○) CC-1.

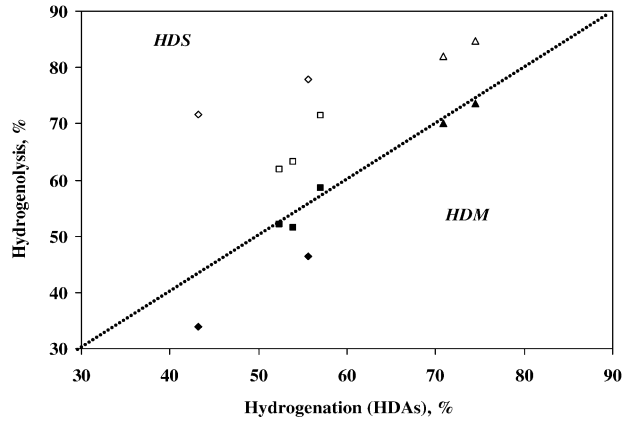

Fig. 6. HDS and HDM selectivities: (△, ▲) CoMo/γ-Al_2O_3-ac; (◇, ◆) NiMo/γ-Al_2O_3-am; (□, ■) CC-1; (open circles HDS and dark circles HDM).

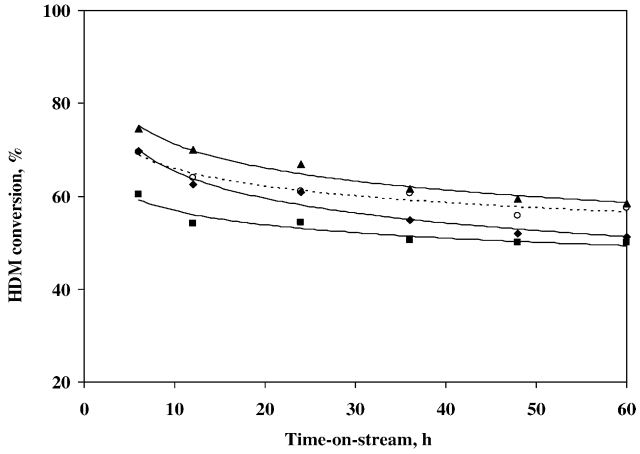

Fig. 7. HDM conversion with time-on-stream: (▲) CoMo/γ-Al_2O_3-acs; (◆) CoMo/γ-Al_2O_3-u; (■) CoMo/γ-Al_2O_3-am; (○) CC-2.

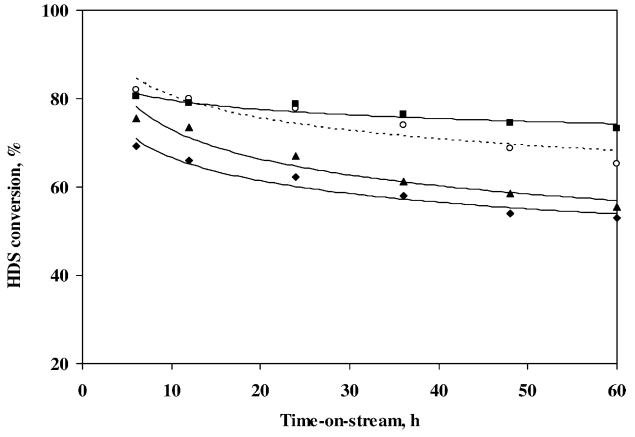

Fig. 8. HDS conversion with time-on-stream: (▲) CoMo/γ-Al_2O_3-acs; (◆) CoMo/γ-Al_2O_3-u; (■) CoMo/γ-Al_2O_3-am; (○) CC-2.

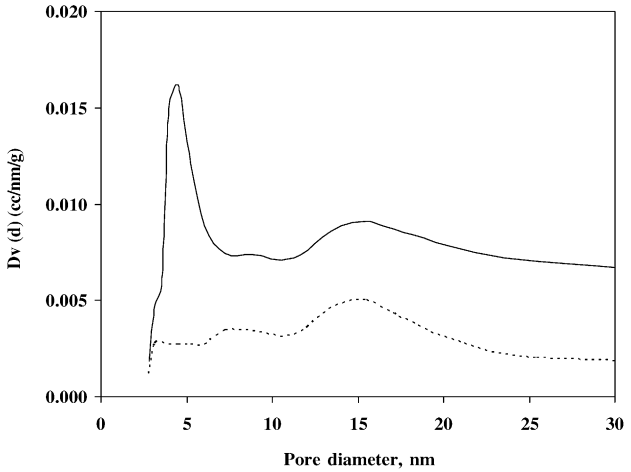

Fig. 9. A comparison of PSD of fresh and spent catalyst: (—) CoMo/γ-Al_2O_3-acs-fresh; (- - -) CoMo/γ-Al_2O_3-acs-spent.

how pore structures are reduced in deactivated catalyst. Using the HDM feed among all lab prepared catalysts containing Co-Mo the activity is slightly better for CoMo/γ-Al_2O_3-acs while smaller pore catalyst (CoMo/γ-Al_2O_3-am) showed lower activity for HDM. Thus, the pore size distributions are in good agreement with HDM conversion. The low conversion in the case of CoMo/γ-Al_2O_3-am is due to its pore distribution in the range of 5–15 nm while the other catalysts have macro-pore size profile in the range of 20–200 nm.

In Fig. 8, the HDS conversion showed opposite trends with respect to HDM which revealed that HDM catalyst should be essentially macro-porous in nature. However, using the less sever HDS feed the pore size distribution does not effect the conversion (Fig. 4) and CoMo/γ-Al_2O_3-am supported catalyst showed much better activity than CC-1. Thus, HDM conversion is limited in the case of CoMo/γ-Al_2O_3-am due to the penetration of porphyrins or metal chelating compounds into the pores.

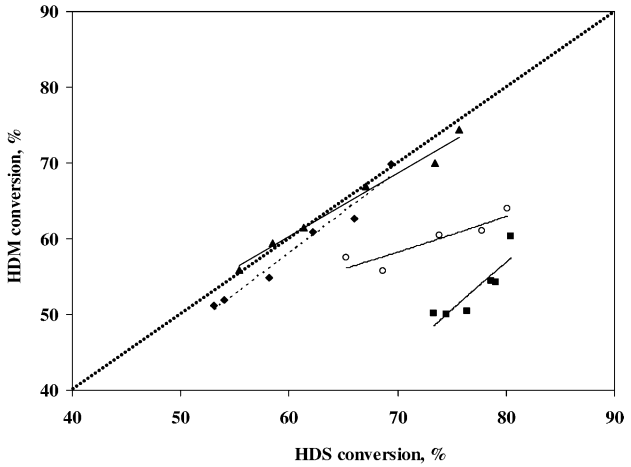

Fig. 10. HDM selectivity: (▲) CoMo/γ-Al_2O_3-acs; (◆) CoMo/γ-Al_2O_3-u; (■) CoMo/γ-Al_2O_3-am; (○) CC-2.

Table 3
Analysis of spent catalysts

Catalysts	Mo (wt.%)	Ni (wt.%)	V (wt.%)	C (wt.%)	S (wt.%)	S/Mo (mol/mol)
HDS feed						
CoMo/γ-Al_2O_3-ac	4.9	0.05	0.19	11.3	5.19	3.1
NiMo/γ-Al_2O_3-am	5.4	2.01	0.13	11.0	4.64	2.5
CC-1[a]	6.7	2.13	0.21	15.6	6.18	2.7
HDM feed						
CoMo/γ-Al_2O_3-u	5.3	0.11	0.69	13.9	5.03	2.8
CoMo/γ-Al_2O_3-acs	4.7	0.11	0.65	16.1	6.23	3.9
CoMo/γ-Al_2O_3-am	5.4	0.08	0.43	10.5	4.45	2.4
CC-2[b]	6.3	2.33	0.45	14.4	6.8	3.2

[a] γ-Al_2O_3 + Ti 5.6 wt.%.
[b] γ-Al_2O_3 + Ti 3.7 wt.%.

The selectivity of HDM is shown in Fig. 10 against HDS. The HDM selectivity is depends mainly upon the greater than 100 nm pores size distribution (Fig. 2a) which decreases in order CoMo/γ-Al_2O_3-acs > CoMo/γ-Al_2O_3-u ≥ CC-2, while CoMo/γ-Al_2O_3-am does not contain more than 50 nm pores. HDM selectivity also followed the same trend. On the other hand the low range pore size distribution catalyst (CoMo/γ-Al_2O_3-am) is highly selective towards the HDS activity.

3.4. Catalysts stability

An important factor which has an immense impact on the economy of catalyst development or stability is the variation of conversion as a function of time-on-stream. The physical characterization results indicated that the smaller the diameter of pores the shorter the life of catalysts. The present results showed that pore volume of the catalyst also affects the catalyst stability. Generally, for heavier feedstocks, the hydrotreating catalysts stability should be directly proportional to the total pore volume and mean radius of the pores. Thus, the stability of catalyst can be drawn using the equation:

$$s = a_1 Vr + b_1 \ (\mathrm{cm}^3/\mathrm{nm/g})$$

where s is the catalyst stability, V the pore volume, r the pore radius and a_1 and b_1 are the constants. This proportionality between the stability of catalyst and the pore volume and radius has been confirmed experimentally by Nomura et al.

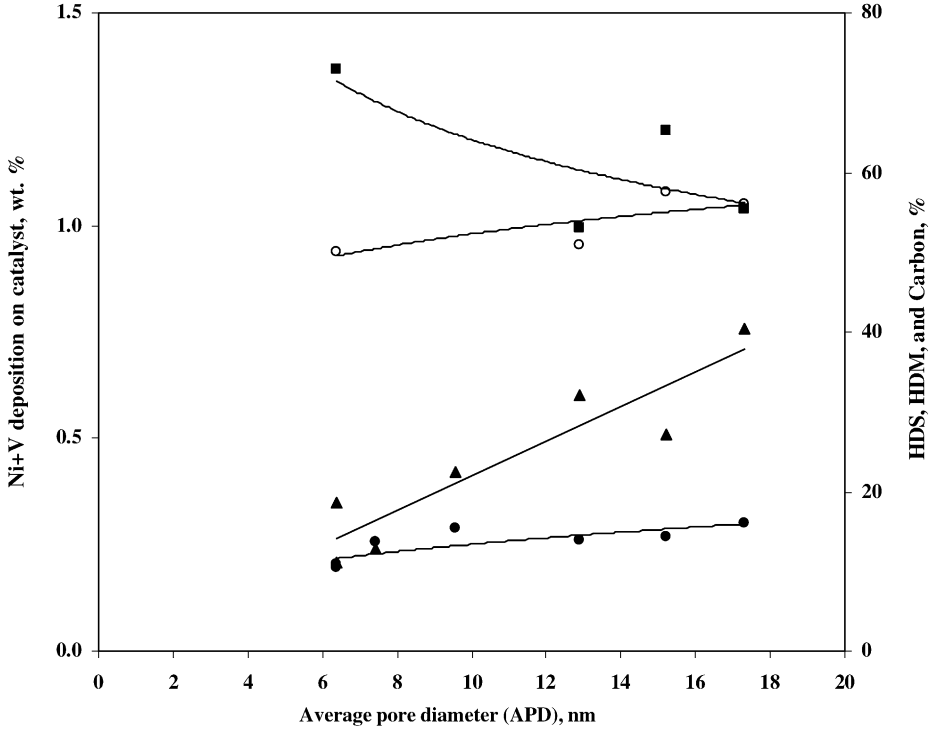

Fig. 11. Effect of average pore size distribution on HDS, HDM conversion and deposition of carbon and metal: (▲) Ni + V; (●) carbon; (■) HDS-60 h; (○) HDM-60 h.

[25,26]. The stability of catalysts is closely related to the metallic (Ni, V, etc.) content, asphaltene and compositions of the feed. The spent catalyst results show that the metallic deposition on the catalyst surface is more of the vanadium metal sulfides that deposited as larger crystallite than nickel. The activity results show that metal deposition increases up to 20–30 h, after that the activity stands more or less constant. However, nickel is much less deposited than vanadium (5–6 times) as can be seen in Table 3. XRD results also support these observations, which indicate that Ni is subtlety distributed on the catalyst surface in comparison with vanadium.

Carbonaceous substances tend to reach their maximum concentration up to 16.1 wt.%, the deposition of carbonaceous substances increases with increasing average pore diameter of catalyst as shown in Fig. 11. Similarly the sulfur content on spent catalysts slightly increases with average pore diameter, however, the mole ratio of S/Mo shows that the higher the average pore diameter the greater the S/Mo ratio, which again indicates that the larger the average pore diameter the greater the stability or metal retention capacity of catalyst. Fig. 11 also shows the HDS and HDM activities against average pore diameter along with metal (V + Ni) deposition on the catalyst after 60 h time-on-stream. In this figure, the HDM activity increases while the HDS activity decreases with increasing average pore diameter. The decreases in HDS activity mean that it is distinctively different from the HDM. Most likely the HDS activity appreciably depends on the surface and active metal sites, while HDM activity depends on the pore size distribution. The working catalyst surface area and pore volume decrease with increasing time-on-stream, after 60 h the pore size distributions are reduced by half or more as shown in Fig. 9. The reasons of decreasing activity are the blocking of active sites and the deposition of carboneous and metallic impurities in the interstices between the catalyst particles. Since stability of catalysts is not an innate property of the catalyst therefore it varies on the type of feed being processed and the operating conditions.

4. Conclusion

Urea hydrolysis ammonium carbonate prepared supports provide better pore size distribution as well as higher pore volume. This method shows larger sol crystallite which leads to an increase in pore size and the corresponding shift toward the average pore diameter along with a corresponding broadening of the pore size distribution. The ammonia prepared support (industrially applicable) only showed meso-pores range of pore size and high surface area. The effect of support preparation on the pore size distribution and average pore diameter apparently control the catalytic activity. During the hydrotreating of heavy Maya crude oil, the HDM and HDAs activities significantly depend on the catalyst pore size distribution while the HDS activity mostly depends on the metal dispersion as well as the high surface area of supported catalysts. Bigger pore size distribution catalysts (CoMo/γ-Al_2O_3-u and CoMo/γ-Al_2O_3-acs) correspond to the better HDM activity and more stability with time-on-stream. However, the study needs more analysis and characterization regarding the above said statement but at the first look pore size distribution well agreed with the activity results.

Acknowledgements

One of us M.S. Rana thanks to Instituto Mexicano del Petroleo (Mexico) for providing PDF. We express our appreciation to Mr. Juan Rangel and Mrs. Bertha Nuñez for helping in preparation of feeds and adsorption–desorption experiments.

References

[1] Energy Information Administration, http://www.eia.doe.gov.
[2] J.W. Gosselink, CatTech 2 (1998) 127.
[3] H. Topsøe, B.S. Clausen, F.E. Massoth, in: J.R. Anderson, M. Boudart (Eds.), Hydrotreating Catalysis–Science, Technology, vol. 11, Springer-Verlag, New York, 1996.
[4] E. Furimsky, F.E. Massoth, Catal. Today 52 (1999) 381.
[5] T.F. Yen, G.V. Chingarian (Eds.), Asphaltene and Asphalts, vol. 1, Elsevier, Amsterdam, 1994, p. 1.
[6] E.Y. Sheu, Energy Fuels 16 (2002) 74.
[7] L. Artok, Y. Su, Y. Hirose, M. Hosokawa, S. Murata, M. Nomura, Energy Fuels 13 (1999) 287.
[8] K.L. Gawrys, P.M. Spiecker, P.K. Kilpatrick, Am. Chem. Soc., Div. Petrol. Chem. 47 (2002) 332.
[9] A. Miyauchi, Y. Inoue, Petrotech 13 (1990) 44.
[10] K. Sakanishi, T. Manabe, I. Watanabe, I. Mochida, J. Jpn. Petrol. Inst. 43 (2000) 10.
[11] S. Terai, H. Fukuyama, K. Uhara, K. Fujimoto, J. Jpn. Petrol. Inst. 43 (2000) 17.
[12] L.C. Castañeda, F. Alonso, J. Ancheyta, Stud. Surf. Sci. Catal. 133 (2001) 477.
[13] S.K. Maity, J. Ancheyta, L. Soberanis, F. Alonso, M.E. Llanos, Appl. Catal. A 244 (2003) 141.
[14] S.K. Maity, J. Ancheyta, L. Soberanis, F. Alonso, Appl. Catal. A 250 (2003) 231.
[15] S.K. Maity, J. Ancheyta, L. Soberanis, F. Alonso, Appl. Catal. A 253 (2003) 125.
[16] K.S.W. Sing, D.H. Everett, R.W.A. Haul, L. Moscu, R.A. Pierotti, J. Rouquerol, T. Siemieniewska, Pure Appl. Chem. 57 (1985) 603.
[17] Powder Diffraction Files, JCPDS, International Central for Diffraction Data, 1969.
[18] B.J. Smith, J. Wei, J. Catal. 132 (1991) 1.
[19] B.J. Smith, J. Wei, J. Catal. 132 (1991) 21.
[20] B.J. Smith, J. Wei, J. Catal. 132 (1991) 41.
[21] C. Takeuchi, S. Asaoka, S. Nakata, Y. Shiroto, Am. Chem. Soc., Prepr. Div. Petrol. Chem. 30 (1) (1985) 96.
[22] H. Toulhoat, J.C. Plumail, C. Houpert, R. Szymanski, P. Bourseau, G. Muratet, ACS Div. Petrol. Chem. Symp. Adv. Reside Upgrading 32 (2) (1987) 463.
[23] S. Eijsbouts, J.J.L. Heinemann, H.J.W. Elzerman, Appl. Catal. A 105 (1993) 69.
[24] S. Eijsbouts, Stud. Surf. Sci. Catal. 127 (1999) 21.
[25] H. Nomura, Y. Sekido, Y. Oguchi, Sekiyu Gakkaishi 23 (5) (1980) 321.
[26] K.L. Kim, K.S. Choi, Int. Chem. Eng. 27 (2) (1987) 340.